ORIGINAL ARTICLE

Identification of syntrophic acetate-oxidizing bacteria in anaerobic digesters by combined protein-based stable isotope probing and metagenomics

Freya Mosbæk[1,3], Henrik Kjeldal[1,3], Daniel G Mulat[2], Mads Albertsen[1], Alastair J Ward[2], Anders Feilberg[2] and Jeppe L Nielsen[1]
[1]Department of Chemistry and Bioscience, Aalborg University, Aalborg, Denmark and [2]Department of Engineering, Aarhus University, Aarhus, Denmark

Inhibition of anaerobic digestion through accumulation of volatile fatty acids occasionally occurs as the result of unbalanced growth between acidogenic bacteria and methanogens. A fast recovery is a prerequisite for establishing an economical production of biogas. However, very little is known about the microorganisms facilitating this recovery. In this study, we investigated the organisms involved by a novel approach of mapping protein-stable isotope probing (protein-SIP) onto a binned metagenome. Under simulation of acetate accumulation conditions, formations of ^{13}C-labeled CO_2 and CH_4 were detected immediately following incubation with [U-^{13}C]acetate, indicating high turnover rate of acetate. The identified ^{13}C-labeled peptides were mapped onto a binned metagenome for improved identification of the organisms involved. The results revealed that *Methanosarcina* and *Methanoculleus* were actively involved in acetate turnover, as were five subspecies of *Clostridia.* The acetate-consuming organisms affiliating with *Clostridia* all contained the FTFHS gene for formyltetrahydrofolate synthetase, a key enzyme for reductive acetogenesis, indicating that these organisms are possible syntrophic acetate-oxidizing (SAO) bacteria that can facilitate acetate consumption via SAO, coupled with hydrogenotrophic methanogenesis (SAO-HM). This study represents the first study applying protein-SIP for analysis of complex biogas samples, a promising method for identifying key microorganisms utilizing specific pathways.
The ISME Journal (2016) **10,** 2405–2418; doi:10.1038/ismej.2016.39; published online 29 April 2016

Introduction

Anaerobic digestion (AD) of organic materials to biogas has several environmental benefits with the methane-rich biogas as a source of renewable energy, as a wastewater treatment technology for the removal of pathogens, as well as odor and pollution reductions from agricultural, industrial and municipal wastes.

The AD of organic matter to biogas involves the coordinated activity of diverse subgroups of highly specialized microbial organisms, hence the stability of AD is highly dependent on the microbial community structure and interactions within the community. Failure to maintain the balance between these groups can lead to reactor inhibitions and

breakdown (Demirel and Yenigün, 2002). Accumulation of volatile fatty acids (VFAs) may cause acidification and result in reduced process performance or worst-case scenario: complete reactor failure (Angelidaki and Ahring, 1993; Chen *et al.*, 2008; Krakat *et al.*, 2011). Accumulation of acetate, an important intermediate VFAs in the anaerobic decomposition of organic matter, has been observed under various operational conditions, and the effects on the microbial community have been addressed in several studies (Palatsi *et al.*, 2011; Fotidis *et al.*, 2013; Lü *et al.*, 2013; Rajagopal *et al.*, 2013; Labatut *et al.*, 2014). Although methanogenesis from acetate (aceticlastic methanogenesis) is fairly well described, less is known about the organisms and metabolisms involved in oxidation of acetate to hydrogen and carbon dioxide (syntrophic acetate oxidation (SAO)) catalyzed by SAO bacteria. The formyltetrahydrofolate synthetase-encoding gene, *fthfs*, is key in the reductive acetogenesis (acetyl-CoA pathway). The enzyme encoded by this gene is also able to catalyze the reverse reaction, oxidizing acetate into H_2 and CO_2 (Xu *et al.*, 2009; Hori *et al.*, 2011). The gene

has therefore been widely used as a biomarker for acetogenesis, although also present in a variety of non-acetogenic bacteria (Lovell and Leaphart, 2005).

Only a few SAO bacterial species have been isolated, and only their genomic potential has been determined (Manzoor *et al.*, 2013; Müller *et al.*, 2013). Isolated synthrophic acetate-oxidizing bacteria (SAOB) cover several bacterial phyla and represent both thermophiles (*Thermacetogenium phaeum* (Hattori *et al.*, 2000); and *Thermotoga lettingae* (Balk *et al.*, 2002)), thermotolerant (*Tepidanaerobacter acetatoxydans* (Westerholm *et al.*, 2011)); and mesophiles (*Clostridium ultunense* (Schnürer *et al.*, 1996); and *Synthrophaceticus schinkii* (Westerholm *et al.*, 2010)). The oxidation of VFAs by syntrophic bacteria is not a thermodynamically favorable process and requires that they are closely associated with methanogens or with non-methanogenic hydrogenotrophs.

Culture-independent approaches using stable isotopes under high levels of acetate revealed high utilization activity of *Methanosarcina* from the archaeal population and putative SAO bacteria affiliating with the *Clostridia* (Hao *et al.*, 2014). Other studies have identified the *Synergistes* group 4 as a major group of acetate-utilizing bacteria in anaerobic sludge batch reactors fed with 2.5–10 mM acetate (Ito *et al.*, 2011).

Protein-stable isotope probing (protein-SIP) can be used to determine not only the identity, but also the activity of active key microorganisms (Jehmlich *et al.*, 2010). Although protein-SIP has been used on other less complex systems (Jehmlich *et al.*, 2008; Bastida *et al.*, 2010; Taubert *et al.*, 2011, 2012; Herbst *et al.*, 2013), it has, as far as we are aware, not been applied on complex environmental samples such as those present in an AD.

In this study, a combination of metagenomics, amplicon sequencing and protein-SIP was used for characterizing acetate-consuming communities in AD. The proteins from actively incorporating organisms were mapped onto a binned metagenome for identification of the bacteria involved. The results obtained in this study indicate SAO bacterial species are important factors in the recovery after acid accumulation, demonstrating the potential of the combined use of metagenomics and protein-SIP as a tool for linking identity and function, as well as providing an understanding of the underlying biology in AD.

Materials and methods

Sources of inoculum

Inoculum was obtained from a commercial full-scale biogas digester at Research Centre Foulum, Denmark. The digester works with a mixture of pig and cattle manure, maize silage and deep litter manure. It is operated under thermophilic conditions (approximately 52 °C). The total solid, volatile solid, pH value and total ammonia nitrogen of the inoculum were 50.2, 40.2, 7.64 and 1.54 g l^{-1}, respectively. The inoculum was starved under anaerobic conditions at 52 °C for 2 weeks before the main tracer experiment to reduce the background contribution of carbon dioxide and methane from the original substrates. A digestate sample was collected at Lynggård biogas plant (11-01-2012), Denmark. Lynggård is operated at 52 °C and runs with pig manure, and grass and maize silage.

Operation of AD

Glass serum bottles (500 ml) were used for preparing the anaerobic incubation assay. Aliquots (195 ml) of inoculum were transferred into the 500 ml serum bottles, which were then sealed with butyl rubber stoppers and aluminum crimps. Five treatments were prepared with [U-^{13}C] and [^{12}C] acetate; detailed information of the reactor setup is summarized in Table 1. For the high-acetate concentration condition, substrate was added at the beginning of the experiment, whereas for the low-concentration condition, substrate was added on a daily basis. All experiments were carried out in triplicate, with the exception of the controls (blank reactors), which were carried out in duplicate. The experiment was run under static incubation conditions for 9 days at 52 °C using strict anaerobic techniques.

Basic analytical methods

The volume of a produced biogas was measured using an acidified water displacement method at room temperature and atmospheric pressure. Headspace biogas was collected using a gas-tight syringe with a needle through a septum and transferred into a 20 ml headspace vial. The compositions of CH_4 and CO_2 in the biogas samples were analyzed by a gas chromatograph 7890A (Agilent Technologies, Horsholm, Denmark) equipped with

Table 1 Description of batch reactors setup

Substrate	Feeding rate
195 ml Inoculum+5 ml water	
195 ml Inoculum+5 ml concentrated CH$_3$COONa to a final of 4 mM acetate	Once at the beginning
195 ml Inoculum+5 ml concentrated CH$_3$COONa to a final of 100 mM acetate	Daily
195 ml Inoculum+5 ml concentrated [U-^{13}C] acetate to a final of 100 mM acetate	Once at the beginning
195 ml Inoculum+5 ml concentrated [U-^{13}C]acetate to a final of 4 mM acetate	Daily

a thermal conductivity detector and a GC sampler 80 (Agilent Technologies).

Liquid samples for VFA analysis were collected periodically and the concentration of VFA determined on a 7890A gas chromatograph (Agilent Technologies), equipped with flame ionization detector. For details of the analysis, refer to Supplementary Methods.

Membrane introduction mass spectrometry measurement

Membrane introduction mass spectrometry was used to monitor the incorporation of ^{13}C into the produced methane and carbon dioxide during the degradation of ^{13}C fully labeled acetate as described elsewhere (Mulat *et al.*, 2014). The membrane introduction mass spectrometry data are reported in terms of atom percent as follows:

$$13X(\text{atom}\%) = \{^{13}X/(^{13}X + ^{12}X)\}, \qquad (1)$$

where ^{13}X represents $^{13}CO_2$ or $^{13}CH_4$, and ^{12}X represents $^{12}CO_2$ or $^{12}CH_4$.

Protein-SIP and amplicon analysis

Liquid samples (5 ml) for protein-SIP and amplicon analysis were collected from all reactors periodically and stored at − 20 °C until analysis. Sampling was performed at 8, 24, 32, 48, 96, 144 and 192 h following the beginning of the experiment. Protein extraction was performed on samples collected at 8, 24, 48 and 192 h using a protocol as previously described (Hansen *et al.*, 2014). Cell debris was removed by centrifugation at 14 500 x*g* for 10 min at 4 °C.

Proteins were acetone precipitated as previously described (Botelho *et al.*, 2010). Precipitated proteins were resuspended in sodium dodecyl sulfate–polyacrylamide gel electrophoresis sample buffer, supplemented with dithiothreitol to a final concentration of 40 m$_M$ and denatured by boiling at 95 °C for 10 min before being loaded onto a pre-cast 4–15% gradient sodium dodecyl sulfate-gel (Bio-Rad, Sundbyberg, Sweden) and separated for 10 min at 160 V.

Liquid chromatography-tandem mass spectrometry

In-gel digestion of proteins was performed as previously described (Shevchenko *et al.*, 2006) and tryptic peptides were analyzed by an automated liquid chromatograph-electrospray ionization tandem mass spectrometer, consisting of an UltiMate 3000 RSLCnano system (Thermo Scientific, Bremen, Germany) coupled to a Q Exactive mass spectrometer (Thermo Scientific) via a Nanospray Flex ion source (Thermo Scientific). The analytical conditions were as previously described (Kjeldal *et al.*, 2014), with the following modifications; analytes were eluted during a 120 min linear gradient, ranging from 12 to 40% (V/V) of solvent B (100% acetonitrile

supplemented with 0.1% (V/V) formic acid) followed by a final step gradient to 90% solvent B which was maintained for 20 min.

Protein analysis

A six-frame translation (every region of DNA has six possible reading frames) and prediction of open reading frames in the in-house constructed metagenome of the anaerobic reactor of Foulum was carried out in MaxQuant v. 1.5.1.2 (Martinsried, Germany). A two-search strategy as previously described was utilized (Seifert *et al.*, 2013). Briefly, an initial survey search was performed, searching against the nonredundant NCBI database, restricting the taxonomy to prokaryota. Sequences that were identified in the survey search were exported from NCBI and merged with the six-frame translation of the metagenome, and the merged database was used in the subsequent main search. For details, refer to Supplementary Methods.

Raw files were analyzed using OpenMS (https://www.openms.de) and the TOPP tools (Kohlbacher *et al.*, 2007; Sturm *et al.*, 2008). RIA and protein LR were, as described elsewhere (Kleindienst *et al.*, 2014). determined using the opensource software OpenMS and the MetaproSIP tool (Sachsenberg *et al.*, 2015).

DNA extraction

DNA extraction was conducted on the liquid biological triplicates collected at 8, 32 and 192 h of incubation periods, using the FastDNA Spin Kit for Soil (MP Biomedicals, Taastrup, Denmark) with minor modifications (for details, refer to Supplementary Methods).

Metagenome preparation

Two metagenomes were prepared from samples collected at the Foulum (13-12-2011) and Lynggård (11-01-2012) biogas plants. DNA was extracted, following a cetyltrimethylammonium bromide and enzyme-based method as described elsewhere (Klocke *et al.*, 2007). DNA was paired-end sequenced (2 × 150 bp) on a Illumina HiSeq2000 (Illumina, Carlsbad, CA, USA), and metagenome reads following analyzed in CLC Genomics Workbench v. 7.03 (CLC Bio, Aarhus, Denmark). For details, refer to Supplementary Methods.

The analysis and binning were performed exactly as described elsewhere (Albertsen *et al.*, 2013). Briefly, the binning of scaffolds to population genomes was performed by plotting the coverage estimates of the metagenomes of Foulum and Lynggard against each other for all scaffolds. Completeness and contamination of six genome bins was evaluated through calculation of GC content, tetranucleotide frequency and by the identification of conserved essential single-copy marker genes.

A detailed description of the approach has been published elsewhere (Albertsen et al., 2013).

Core genes of the Wood–Ljungdahl pathway were searched against the metagenome using Hidden Markov model profiles of these genes downloaded from protein family domains (Pfams) homepage (http://pdam.xfam.org/; Finn et al., 2014) and HMMER3 package (http://hmmer.janelia.org/). For details, refer to Supplementary Methods.

Amplicon sequencing
Materials and methods of amplicon sequencing are provided in Supplementary Methods.

Data availability
All amplicon data are available at European Nucleotide Archive (ENA) under accession number PRJEB10871. Metagenomes and assemblies, and bin genomes are available at ENA under accession number PRJEB10932. The mass spectrometry proteomics data have been deposited at ProteomeXchange Consortium (Vizcaíno et al., 2014) via the PRIDE partner repository with the data set identifier PXD002996.

Results

Degradation of acetate and methane production
Batch reactors inoculated with anaerobic digester sludge were fed two different concentrations of labeled acetate, and the concentration of acetate as a function of time was monitored (Figure 1). The degradation of acetate in the blank reactor (inoculum only) and in the reactors fed with low (4 mM) and high (100 mM) concentrations of [U-^{13}C]acetate were significantly different; the background concentration of acetate in the blank reactor remained at ~ 2 mM for the first 48 h and declined to below the detection limit between 48 and 72 h. No acetate accumulation was observed in reactors fed with low acetate concentration, and the total turnover of acetate was

approximately 2.95 g l^{-1} during the 9 days of incubation.

A continuous turnover of acetate occurred in the high acetate concentration-fed reactor, and the total turnover of acetate was around 8.2 g l^{-1} (acetate was spiked in at the beginning of the experiment only). The degradation of acetate in the high concentration-fed reactor started immediately and followed a linear trend during the first 120 h (corresponding to a consumption of ~ 83% of the amended [U-^{13}C] acetate). After 120 h, the turnover of [U-^{13}C]acetate decreased and finally reached a stationary level during the last 68 h of the incubation. Following 9 days of incubation, the concentration of acetate reached ~ 1.6 mM.

Besides the degradation of acetate, the production of labeled and unlabeled methane and carbon dioxide, respectively, was also monitored (Figure 2). In the low acetate concentration-fed reactor, the proportion of the $^{13}CO_2$ produced to total carbon dioxide increased almost linearly from 6 atom% up to 32 atom% during the 9 days of incubation, whereas the proportion of the $^{13}CH_4$ produced to total methane increased gradually from 45 atom% up to 76 atom%.

In the high acetate concentration-fed reactor, the production of $^{13}CO_2$ increased from 20 atom% to about 45 atom% at 96 h and later stabilized at this value. The production of $^{13}CH_4$ reached the peak value (80 atom%) at 24 h and remained almost stable for 96 h before starting to decline. During the time at which the levels of $^{13}CH_4$ appeared to remain constant (Figure 2), almost 83% of the acetate was degraded (Figure 1). The isotopic abundance of ^{13}C-labeled CO_2 and CH_4 at both low and high concentrations of ^{13}C-labeled acetate incubations indicate the uptake and turnover of the added ^{13}C-labeled acetate.

Phylogenetic microbial community composition of acetate-fed reactors
The microbial community compositions were evaluated by amplicon sequencing of triplicate reactors
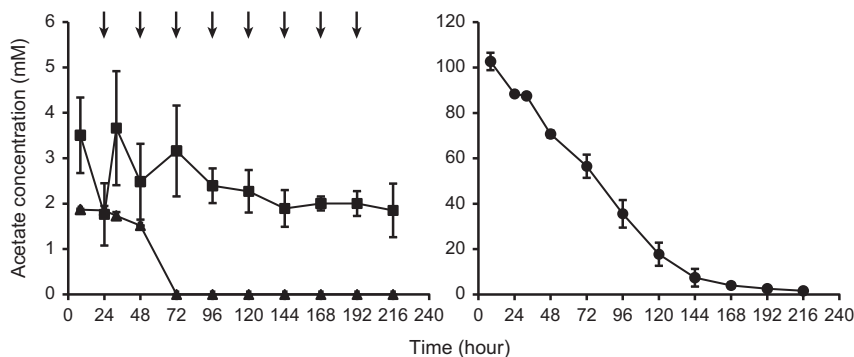

Figure 1 Temporal change of the residual acetate in (**a**) the blank reactors (▲); reactors fed with low concentration (4 mM) of [U-^{13}C] acetate (■); and (**b**) reactors fed with high concentrations (100 mM) of [U-^{13}C]acetate (●). The lines represent mean values (n = 3), and error bars denote the standard deviation. Arrows indicate addition of acetate.
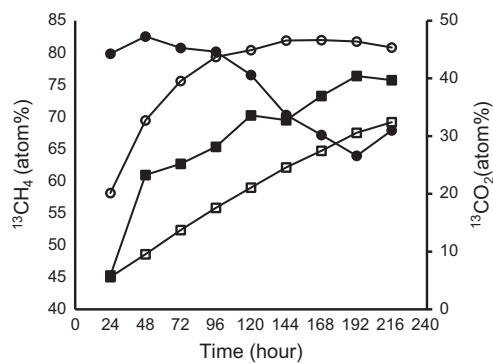
Figure 2 Temporal change of the atom percent of $^{13}CO_2$ and $^{13}CH_4$ in the reactors fed with low concentrations of [U-^{13}C]-acetate (■ $^{13}CH_4$; □ $^{13}CO_2$); and in the reactors fed with high concentrations of [U-^{13}C]acetate (● $^{13}CH_4$; ○ $^{13}CO_2$). The lines represent mean values ($n = 3$), and error bars denote the standard deviation.

fed with low and high concentrations of acetate, respectively, see Supplementary Information. Samples at three time points were chosen for amplicon sequencing (8, 32 and 192 h). At least 29 428 sequences per sample passed filtering. From the archaeal population, the most abundant genera were affiliated with *Methanobacterium*, *Methanosarcina*, *Methanobrevibacter* and *Methanoculleus*. However, *Methanomassiliicoccus* and *Methanothermobacter* were also detected. The five most abundant classes of bacteria belonged to *Clostridia*, *Bacteroidia*, *Bacilli*, *Thermotogae* and *Anaerolineae* (Supplementary Figure 1).

Among abundant genera (>0.1% of the total reads), several genera from the bacterial population were seen to either decrease or increase from 8 to 192 h (Supplementary Figure 1A). The most noticeable change in the microbial community seems to occur among the two orders of *Firmicutes*, *Bacillales* (increasing), and *Clostridiales* (decreasing). The differences in the microbial communities in the high and low acetate time series, as well as the three replicates are illustrated by non-metric multidimensional scaling analysis (Supplementary Figure 1B). The findings revealed high reproducibility of the biological replicates and changes between the time series of each experiment.

Protein-SIP analysis
Time-resolved protein-SIP analysis showed that ^{13}C was incorporated into peptides for the reactor fed with 100 mM [U-^{13}C] acetate, starting from 48 h (Table 2, Figure 3). No ^{13}C labeling was detected in the reactor fed with 4 mM [U-^{13}C]acetate, control (fed with unlabeled acetate) and blank reactors at any time point (data not shown).

In the reactor fed with high concentration of acetate, a total of five peptides incorporated ^{13}C at 48 h (Table 2) after the start of the incubation. From these ^{13}C-labeled peptides, one of them were

assigned to the domain of bacteria and the other two to the domain of archaea. The last two peptides could not be assigned to any sequence present in either of the two metagenomes. A functional annotation was given to three of the peptides. The two peptides belonging to *Archaea* were identified as different subunits of the methyl coenzyme M reductase, a key enzyme involved in methane formation from methanogens (Ermler, 1997). The third peptide, which was unassigned, was identified as flagellin subunit B and is thus related to motility.

Following 192 h, a total of 56 peptides could be identified that showed incorporation of ^{13}C (Figure 3 and Table 2). These peptides were dominated by bacterial species (*Clostridia*). Three labeled peptides originated from the domain of *Archaea* (two from the genus of *Methanoculleus* and one peptide from *Methanosarcina barkeri*). The proportion of the ^{13}C-labeled peptides, known as relative isotope abundance (RIA), as well as how much of a peptide population is labeled, LR, is noted in Table 2. An example of the development of labeling from 24 to 192 h is given in Figure 3b, for a methyl coenzyme M reductase (chain B) from *Methanosarcina barkeri*.

A functional annotation could be assigned for 6 out of the 56 peptides found at 192 h (Figure 3a, Table 2). The remaining five peptides came from proteins from *Clostridia* (four peptides) and an unassigned peptide and had household functions, for example, initiation of RNA synthesis, signal transduction and transport substrate binding. However, one peptide belonged to putative TetR family, which is associated with antibiotic resistance.

The two metagenomes from Foulum and Lynggård biogas plants were sequenced to yield a total of 130 190 434 and 79 999 986 reads, respectively. When assembled, this amounted to a size of 165 123 257 bp for the Foulum metagenome, whereas the Lynggård metagenome was 82 793 162 bp. Both of the metagenomes represent approximately 98% *Bacteria* and 2% *Archaea* (Supplementary Figure 2). The two metagenomes were binned, based on the coverage and scaffold length, and the phylogeny from BLAST of each scaffold was superimposed (Figure 4a). The two metagenomes are relatively similar and were used as a reference database for the identified and ^{13}C-labeled peptides (Figure 4b). The phylogenetic identification in the two metagenomes resembles the phylogenetic identification found by amplicon sequencing (Supplementary Figure 2). Protein-SIP data were superimposed onto the metagenome and all scaffolds belonging to a genome bin for which labeling of proteins were observed were extracted. The scaffolds of a total of six genome bins were extracted and completeness and potential contamination of each genome bin was evaluated (Table 3). The details of the assembly can be found in the Supplementary File 1.

Table 2 Peptides for which an increase in isotopic incorporation of ¹³C was observed in the reactor fed with 100 mM [U-¹³C]acetate

Accession[a]	Peptide sequence[b]	Description[c]	Exp. m/z[d]	Theo. m/z[e]	Z[f]	RIA 1[g]	RIA 2[h]	LR[i]	Taxonomy[j]
48 h									
GI|219919005|	GPNEPCGLSFGHLSDIIQTSR	Methyl coenzyme M reductase subunit alpha	728.0337	728.0344	3	1.2	51.1	7.4	Archaea
3291:TRUE:2282	LIGHGPFILDQYK		500.9459	500.9452	2	0.6	25.1	0.8	*Clostridia* (C2) (genus *Gelria*)
GI|115144434|	SVAVNLAGIQGALASGK	Chain B, Methyl-Coenzyme M Reductase	778.4442	778.4438	2	0.6	57.6	5.8	*Methanosarcina barkeri*
2256:TRUE:10376	AGDDAAGLSISEK	Flagellin, subunit protein B	617.3017	617.3015	2	0.6	90.3	91.3	Unassigned
40545:TRUE:0	LTPEEFVSTFIPADLTWM(Oxidation)R		757.0406	757.0452	3	1.1	14.0	60.6	Unassigned
192 h									
16:FALSE:5223	AILPSPYGAFTR		646.8548	646.8535	2	0.6	32.2	10.7	*Clostridia* (C1) (genus *Gelria*)
1400:FALSE:7184	VDELLELGR		522.2914	522.2902	2	0.7	31.7	26.1	*Clostridia* (C1) (genus *Gelria*)
18:FALSE:4093	FQVGFEEGVK	ABC transporter substrate-binding protein	570.2911	570.2902	2	0.6	30.4	9.9	*Clostridia* (C1) (genus *Gelria*)
2364:FALSE:3984	DNPESIFVPLPIVIDPLVEER		797.7637	797.7651	3	1.2	28.4	12.2	*Clostridia* (C1) (genus *Gelria*)
34:TRUE:27427	QIVGELFQEDLAALGIK		922.5129	922.5118	2	1.2	27.8	9.3	*Clostridia* (C1) (genus *Gelria*)
8772:TRUE:988	ELLAEAGIEPGEISIR		848.9621	848.9594	2	1.2	27.5	6.2	*Clostridia* (C1) (genus *Gelria*)
515:TRUE:2	IEVTVEEGLPVAK		692.3909	692.3901	2	0.6	26.9	13.9	*Clostridia* (C1) (genus *Gelria*)
888:FALSE:1680	AAELGVTLR	Signal transduction histidine kinase-like protein	465.2752	465.2744	2	0.7	26.8	6.2	*Clostridia* (C1) (genus *Gelria*)
448:TRUE:12186	ALAFAVNPEIIVER		771.4387	771.4379	2	0.6	26.6	7.9	*Clostridia* (C1) (genus *Gelria*)
515:TRUE:2	RGEIGGTIR		544.2969	544.2964	2	0.7	26.6	10.4	*Clostridia* (C1) (genus *Gelria*)
448:TRUE:12186	AIGINANPAFPDAGVYNDR		987.9882	987.9871	2	1.2	26.3	17.6	*Clostridia* (C1) (genus *Gelria*)
34:TRUE:27427	IDEVWLAAQR		600.823	600.8222	2	0.6	25.9	19.6	*Clostridia* (C1) (genus *Gelria*)
515:TRUE:2	RGEIGGTIR		544.2968	544.2964	2	0.7	25.8	0.9	*Clostridia* (C1) (genus *Gelria*)
447:FALSE:10792	SGAQVLLSR		465.7724	465.772	2	0.6	25.5	5.9	*Clostridia* (C1) (genus *Gelria*)
515:TRUE:2	AGELAFSASK		490.7562	490.756	2	0.7	25.4	16.8	*Clostridia* (C1) (genus *Gelria*)
73:FALSE:5845	DFPLYGAGDRTEDNLIK		641.9862	641.9864	3	1.2	25.4	13.6	*Clostridia* (C1) (genus *Gelria*)
34:TRUE:27427	IDQELILVR		549.8302	549.8295	2	0.7	25.1	11.0	*Clostridia* (C1) (genus *Gelria*)
2364:FALSE:3984	GVIDPETFILNYDQYIEK		1079.043	1079.041	2	1.2	25	13.9	*Clostridia* (C1) (genus *Gelria*)
2074:TRUE:5302	IDSDLSKYDVYLQSAAR		648.6618	648.6618	3	1.2	24.8	22.0	*Clostridia* (C1) (genus *Gelria*)
54:TRUE:1185	LELLINENR		557.3177	557.3168	2	0.7	24.5	2.4	*Clostridia* (C1) (genus *Gelria*)
73:TRUE:13399	VYYALDEPQAINALR		868.4566	868.4543	2	1.2	24.5	7.8	*Clostridia* (C1) (genus *Gelria*)
109:TRUE:9954	ITTTDINDVAHHQFK		438.7331	438.7323	4	1.2	24.2	18.4	*Clostridia* (C1) (genus *Gelria*)
515:TRUE:2	FITVGEKYPEGLTAPR		593.3216	593.321	3	1.2	24	18.7	*Clostridia* (C1) (genus *Gelria*)
448:TRUE:12186	TLDLSNYFIPGVPAIK		874.4877	874.4851	2	1.5	23.7	9.1	*Clostridia* (C1) (genus *Gelria*)
34:TRUE:27427	NDNYYEFDEEGNRLPYLNR		807.6958	807.6963	3	1.2	23.1	12.2	*Clostridia* (C1) (genus *Gelria*)
109:TRUE:9954	ITTTDINDVAHHQFK		584.6417	584.6407	3	1.2	22.8	17.4	*Clostridia* (C1) (genus *Gelria*)
139:FALSE:61670	TLDEFFQIAK		606.3202	606.319	2	0.6	22.3	38.3	*Clostridia* (C1) (genus *Gelria*)
49:TRUE:24338	DLFVQAGLPTPNELQNEGR		1049.533	1049.532	2	1.2	21.7	22.9	*Clostridia* (C1) (genus *Gelria*)
515:TRUE:2	GFVSNPYTGNYM(Oxidation)PHR		585.9351	585.9351	3	1.2	21	20.7	*Clostridia* (C1) (genus *Gelria*)
1400:FALSE:7184	AVTGPLPPLVWASR		732.4232	732.4221	2	0.6	20.7	21.6	*Clostridia* (C1) (genus *Gelria*)
515:TRUE:2	GFVSNPYTGNYM(Oxidation)PHR		585.9357	585.9351	3	1.2	20.7	13.4	*Clostridia* (C1) (genus *Gelria*)
34:TRUE:27427	EYEISEDGTEVTFYLR		975.9533	975.952	2	1.3	20.3	14.7	*Clostridia* (C1) (genus *Gelria*)
73:FALSE:5845	YNVEVEFKPVPR		492.9338	492.933	3	0.6	20.3	12.9	*Clostridia* (C1) (genus *Gelria*)
448:TRUE:12186	AIGINANPAFPDAGVYNDR		658.9934	658.9938	3	1.2	15	7.1	*Clostridia* (C1) (genus *Gelria*)
448:TRUE:12186	DDNWWGNAVFGQPKPK		620.3004	620.3006	3	1.2	13.6	11.4	*Clostridia* (C1) (genus *Gelria*)
2250:TRUE:7164	FVAIEHVSADAAR		462.5779	462.5772	3	0.7	93.8	35.0	*Clostridia* (C2) (genus *Gelria*)
3291:TRUE:2282	QAADEAQLILAR		649.8583	649.8568	2	0.6	36	9.0	*Clostridia* (C2) (genus *Gelria*)
1633:FALSE:12343	LLIALQTSDK		551.3309	551.3293	2	0.7	34.3	21.4	*Clostridia* (C2) (genus *Gelria*)
3291:TRUE:2282	LLDEAGYTVDPATGIR		845.9382	845.936	2	0.7	32.2	7.0	*Clostridia* (C2) (genus *Gelria*)
862:TRUE:2131	IAIVFATCGLGDK		631.3625	631.3612	2	0.6	30.5	8.1	*Clostridia* (C2) (genus *Gelria*)
3291:TRUE:2282	REPLADDVLR	Putative TetR family transcriptional regulator	592.3258	592.3251	2	0.7	30.1	5.9	*Clostridia* (C2) (genus *Gelria*)
709:TRUE:15243	HFTNSIRPIR		414.2352	414.2352	3	0.6	28.9	13.9	*Clostridia* (C2) (genus *Gelria*)
3291:TRUE:2282	LIGHGPFILDQYK		500.9458	500.9452	3	0.6	26.2	6.1	*Clostridia* (C2) (genus *Gelria*)
3291:TRUE:2282	WTTLNIKPVR		409.912	409.9118	3	0.6	24.6	6.5	*Clostridia* (C2) (genus *Gelria*)

Table 2 (Continued)

Accession[a]	Peptide sequence[b]	Description[c]	Exp. m/z[d]	Theo. m/z[e]	Z[f]	RIA 1[g]	RIA 2[h]	LR[i]	Taxonomy[j]
709:TRUE:15243	NLTFAEVGFR	Simple sugar transport system substrate-binding protein	577.3048	577.3037	2	0.7	17.3	8.8	Clostridia (C2) (genus Gelria)
1006:TRUE:9099	VVEAAIAAGK		464.7768	464.7767	2	0.7	30.9	12.6	Clostridia (C3)
1279:TRUE:16513	AIISVDANTQSHGVVIR		593.996	593.9952	3	1.3	27.2	17.6	Clostridia (C3)
1279:TRUE:16513	VAIGVEDLGHTSLAER		556.2979	556.2968	3	1.2	26.8	15.0	Clostridia (C3)
2799:FALSE:25402	IFTVDQISFIPK		704.3993	704.3978	2	0.6	21.4	9.5	Clostridia (C4)
2799:FALSE:25402	ALELSLEDSPR		615.323	615.3222	2	0.6	20.7	5.0	Clostridia (C4)
527:FALSE:43604	VLELALKDSVR		414.9192	414.9187	3	0.6	23.9	17.7	Clostridia (C5)
2628:TRUE:10590	ELDLDIVGNKDAVISK		576.9853	576.9841	3	1.2	51.7	2.8	Methanoculleus
2628:TRUE:10590	TIAVNLGGIEGALK		678.3993	678.3983	2	0.6	49.6	2.3	Methanoculleus
GI 11514434|	SVAVNLAGIQGALASGK	Chain B, Methyl-Coenzyme M Reductase	778.445	778.4438	2	0.6	58.1	39.2	Methanosarcina barkeri
33816:FALSE:2321	ILDLLDSAPDLATAK		778.4337	778.4325	2	1.2	31.9	14.9	Unassigned
GI 652561026|	EIALSLDLSPR	RNA polymerase sigma-70 factor, expansion family 1	607.3438	607.343	2	0.7	24.4	15.4	Unassigned

[a]Protein identifier from metagenome or gene identifier (GI) for the corresponding protein. [b]Peptide sequence (with identified modification). [c]Description of the identified protein. [d]Experimentally determined mass-to-charge ratio of the observed sequence. [e]Theoretically determined mass-to-charge ratio of the observed sequence. [f]Charge of the tryptic peptide. [g]Relative isotope abundance of the naturally occurring isotopic cluster of the peptide. [h]Relative isotope abundance of isotopic cluster of the peptide showing incorporation of ^{13}C. [i]Labeling ratio. [j]Highest possible taxonomic classification.

The Wood–Ljungdahl pathway has four marker genes, *acsB* (carbon monooxide dehydrogenase), the two subunits of the corrinoid iron sulfur protein (*acsC* and *acsD*), and *ftfhs* (formyltetrahydrofolate synthatase) (Can *et al.*, 2014). Searching Hidden Markov model profiles of each of the functional domains of these marker proteins against the six-frame translated metagenome, revealed that all of the six *Clostridia* bin genomes contained the *ftfhs* gene, whereas genes *acsC* and *acsD* were only found in one of the bin genomes (*Clostridia* (C4). All of the six genome bins tested positive for all the genes of the Wood–Ljungdahl pathway (Supplementary File 2).

Eleven proteins from a syntrophic glutamate-oxidizing bacterium of the genus *Gelria* (C2) were labeled with ^{13}C during the SIP experiment (Table 2). The genus *Gelria* (phylum *Clostridia*) (C1) was the most heavily labeled in the proteome with 35 ^{13}C-labeled peptides.

Gelria belongs to the family *Thermoanaerobacteraceae* and is closely related to the genus of two of the known SAOB, namely *Thermacetogenium phaeum* and *Tepidanaerobacter acetatoxydans*, which are also part of the *Thermoanaerobacteraceae* family. *Thermacetogenium* had a relative read abundance of 0.01–0.11% in the amplicon data. Overall, the *Thermoanaerobacteraceae* family was found with an abundance of 0.8–2.0% in the different batch samples. Several *ftfhs* genes from *Clostridia* were found in the six-frame translated metagenome of the Foulum plant (Supplementary File 2).

Thermotoga lettingae is another known SAOB in the family *Thermotogaceae*. We did not detect any labeling in the proteins of this organism. A closely related genus, S1, was highly abundant in the amplicon data with a relative abundance of 2.1–7.2%. FTFHS was observed in *Thermotogae* in the six-frame translated metagenome (Supplementary Figure 1).

Six proteins from *Clostridia* were ^{13}C labeled, but not found in any of the bins and could not be identified at a higher taxonomic level. Amplicon sequencing revealed that the genus *Clostridium* had a relative abundance of 0.6–1.4%. However, the known SAOB, *Clostidium ultunese,* was not detected with ^{13}C incorporation, nor in the amplicon and metagenome data. Furthermore, *Syntrophaceticus schinkii*, from the family *Thermoanaerobacterales* Family III, order *Thermoanaerobacterales*, which is the last of the known SAOB, was not identified from the SIP experiment, nor was this family detected with amplicon sequencing.
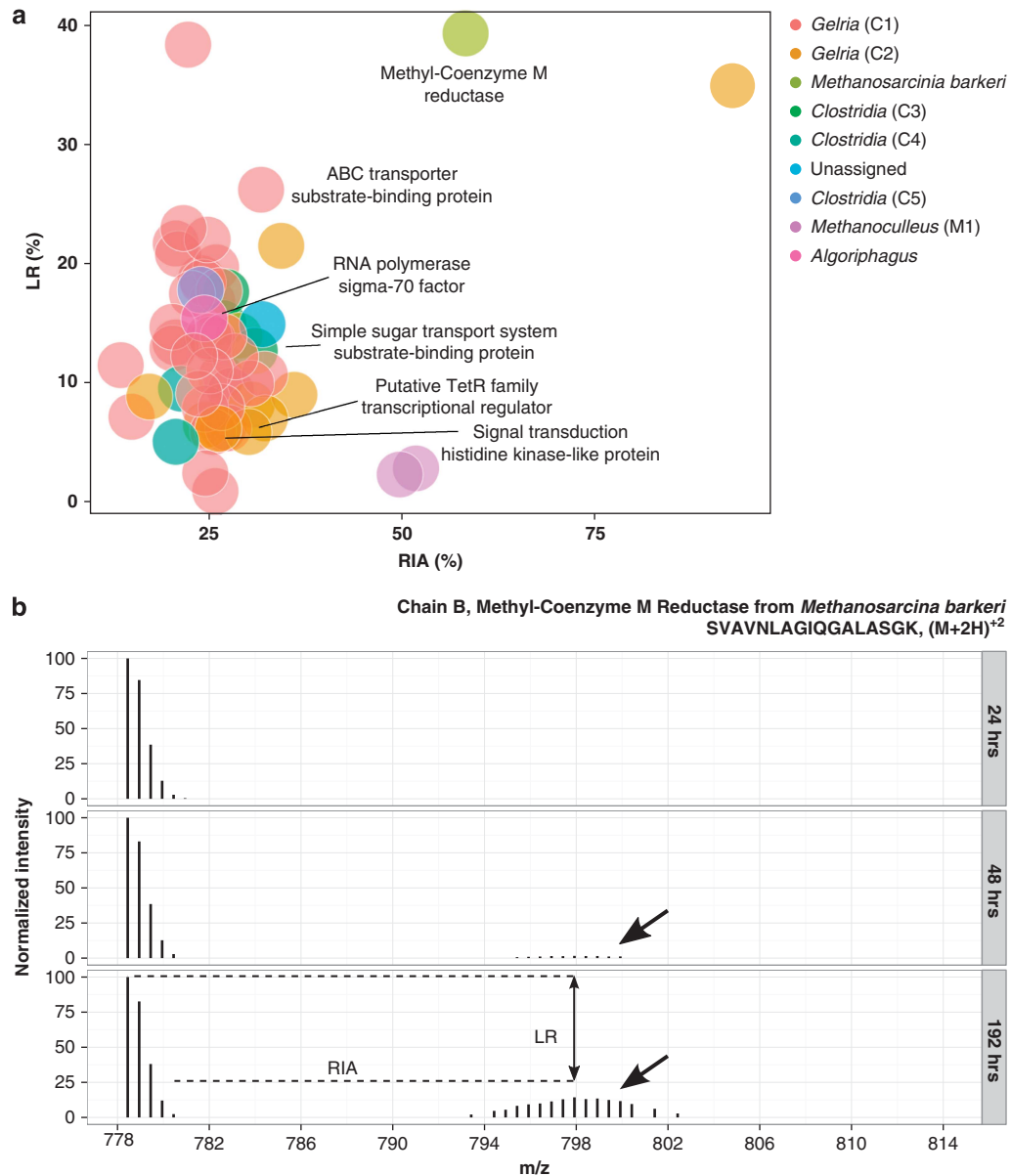
Discussion

Our aim was to apply protein-SIP to describe the complex system of AD. Peptides showing incorporation of ^{13}C were mapped onto a binned metagenome in order to identify key microorganisms involved in

Figure 3 (**a**) RIA as a function of LR for peptides, showing incorporation of ^{13}C at 192 h in the reactor fed with 100 mM of [U-^{13}C]acetate (colors represent highest possible taxonomic rank with names in brackets corresponding to extracted genome bins). Functionally annotated proteins are indicated in the figure. The peptide SVAVNLAGIQGALASKGK, which showed a high degree of ^{13}C incorporation, was identified belonging to *Methanosarcina barkeri*. (**b**) Time resolved analysis of the incorporation of ^{13}C in the peptide SVAVNLAGIQGALASKGK belonging to the methanogenic archaea *Methanosarcina barkeri*. Incorporation of ^{13}C in the peptide was evident after 48 h (the arrows indicate the ^{13}C-labeled isotopologue). The peptide was identified as a methyl coenzyme M reductase, which catalyzes anaerobic oxidation of methane. Besides the methyl coenzyme M reductase, proteins with functions related to transport of substrate and sugars, signal transduction, translation as well as a transcriptional repressor were also identified (Figure 3 and Table 2).

recovery of acetate accumulation under conditions simulating normal running conditions (low acetate levels) and stressed conditions with high levels of acetate.

The ^{13}C isotopic profiling during the start of incubation in both the low and high concentrations of [U-^{13}C]acetate showed that CO_2 and CH_4 are the main products of acetate degradation. As both the methyl and carboxyl groups are ^{13}C labeled in the [U-^{13}C]acetate, it is difficult to estimate the proportion of methane produced through SAO-HM, using the values of atom percent of $^{13}CO_2$ and $^{13}CH_4$. The $^{13}CO_2$ formed can be produced either through acetoclastic methanogenesis or through SAO during the degradation of [U-^{13}C]acetate. In a previous study, performed on sludge from the same plant as

that analyzed in this study, methyl ^{13}C-labeled acetate ([2-^{13}C]acetate) was used to trace incorporation of ^{13}C into CO_2 and CH_4 in real time during the degradation of [2-^{13}C]acetate. The results showed that SAO-HM had a key role in the conversion of acetate to methane as $^{13}CO_2$ can be produced from
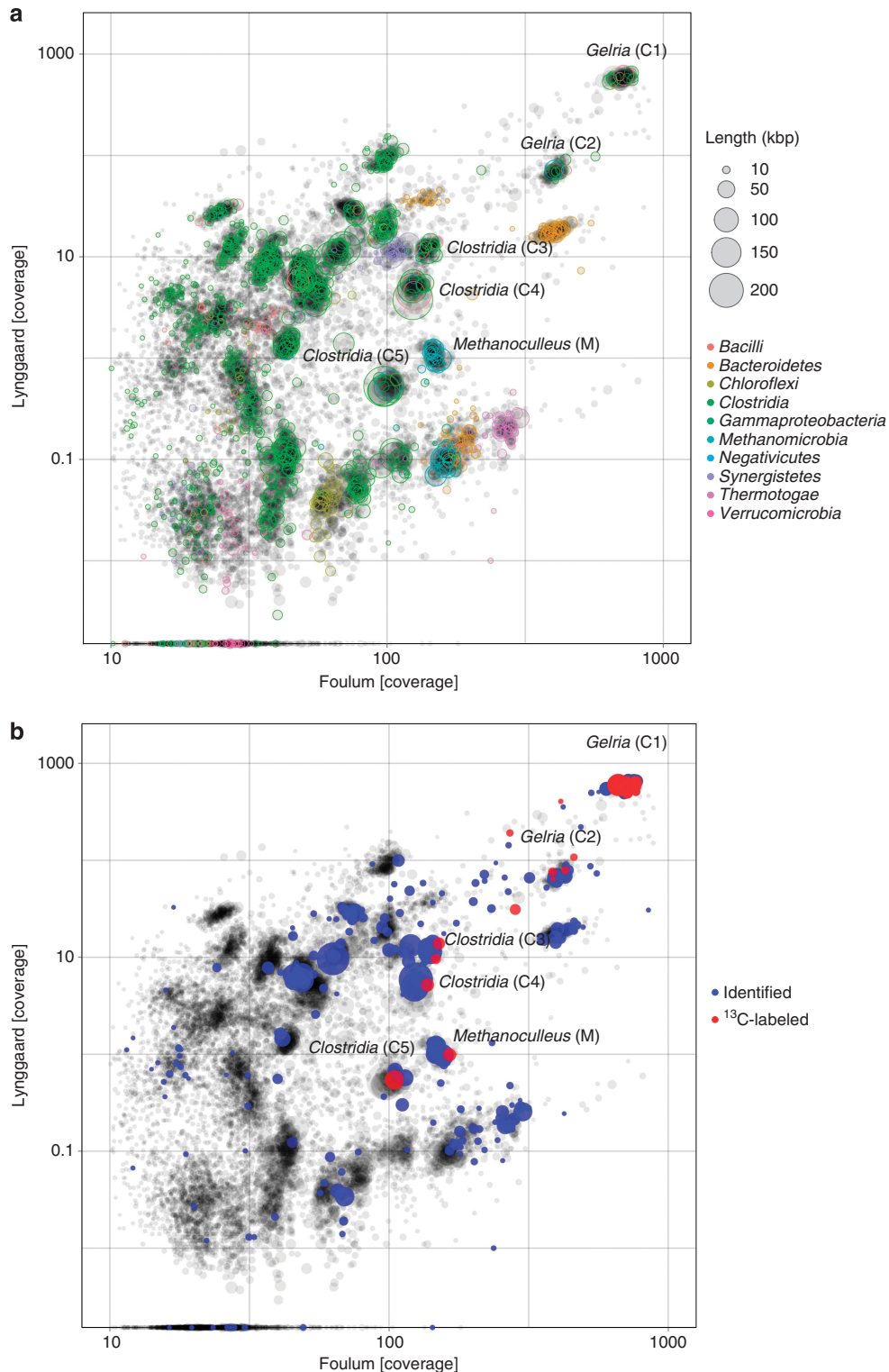

Figure 4 The scaffold coverage from two metagenomes are plotted. The dot sizes indicate the scaffold length. (**a**) Coloring is according to phylogeny. (**b**) Coloring is observed in the protein-SIP analysis according to identified and ^{13}C-labeled peptides. Labeling was seen in six clusters of scaffolds belonging to five subspecies of *Clostridia* and *Methanoculleus*.

Table 3 Assembly statistics of the six genome bins containing scaffolds to which proteins showing incorporation of ^{13}C mapped to in the protein-SIP analysis

Phylogenetic affiliation	No. of contigs	Total length (bp)	GC (%)	N50	Foulum coverage	Lynggaard coverage	No. essential unique genes	No. of total essential genes	Figure 4a
Clostridia (*Gelria*)	128	2 092 416	59.40	25 636	731.79	593.5	104	107	*Gelria* (C1)
Clostridia (*Gelria*)	306	1 833 135	49.50	11 477	405.00	71.02	94	95	*Gelria* (C2)
Clostridia	145	1 786 211	56.90	19 622	140.58	12.09	100	103	*Clostridia* (C3)
Clostridia	71	2 167 847	53.80	71 792	125.47	4.93	102	104	*Clostridia* (C4)
Clostridia	59	2 188 512	53.60	61 047	102.11	0.54	100	103	*Clostridia* (C5)
Methanomicrobia (*Methanoculleus*)	161	2 200 216	59.40	24 804	148.67	1.09	33	35	*Methanoculleus* (M)

The number of essential genes was evaluated using 107 Hidden Markov models of protein coding-essential single-copy genes.

the degradation of [2-^{13}C]acetate through SAO-HM alone (Mulat *et al.*, 2014). Similar observations have been reported after amendment of [2-^{14}C]acetate in batch incubations inoculated with manure and food waste (Karakashev *et al.*, 2006).

A qualitative interpretation of the measured atom percent of $^{13}CH_4$ and CO_2 during the degradation of [U-^{13}C]acetate revealed that the atom% of $^{13}CO_2$ was generally lower than that of the $^{13}CH_4$ in both the low and high concentrations of [U-^{13}C]acetate. This is most likely due to the high background pool of unlabeled CO_2 in the system.

This is corroborated by the levels of $^{13}CH_4$, which reached a maximum of 75 atom% and 80 atom% in the low- and high-acetate-fed reactors, respectively. The production of unlabeled CH_4 is possibly caused by a reduction of the background pool of unlabeled CO_2 by hydrogenotrophs in syntrophy with SAOB. This assumption is in line with previous findings from the same AD, where SAO-HM was found to have a key role for the production of methane during the degradation of high concentrations (100 mM) of [2-^{13}C]acetate (Mulat *et al.*, 2014). Experimental conditions in this study and the previous study (Mulat *et al.*, 2014) were very similar with the exception of the inoculum, which were a few months apart from the same full-scale biogas plant (Foulum). Although fluctuations in community dynamics are expected over time, the community structure between the time of the present and previous studies remained relatively stable (Mulat *et al.*, 2014). The dominant microbial communities are almost similar in both studies (see the discussion below), indicating that SAO-HM had a significant role in the reactor fed with the high concentration of [U-^{13}C]acetate.

The effect of the experimental design on the microbial community composition was investigated by amplicon sequencing of the 16S ribosomal RNA gene in both low- and high-acetate-fed reactors (see Supplementary Information). In general, the microbial communities observed in both batch reactors are in accordance with previous studies of AD communities (Lee *et al.*, 2012; Wirth *et al.*, 2012; Sundberg *et al.*, 2013; St-Pierre and Wright, 2014). The majority of the organisms identified were

affiliated to *Clostridia*. *Clostridia* participate in various stages in AD, including hydrolysis of cellulosic plant biomass and acetate oxidation (Hattori, 2008; Schlüter *et al.*, 2008; Wirth *et al.*, 2012). The bacterial classes of *Bacteroidia*, *Bacilli*, *Thermotogae*, *Anaerolineae*, *Synergistia*, as well as several *Proteobacteria* were also highly abundant. This composition is also in accordance with our metagenome constructed from the Foulum and Lynggaard biogas plants. *Methanobacterium*, *Methanosarcina*, *Methanobrevibacter* and *Methanoculleus*, representing hydrogenotrophic and acetoclastic methanogens, were present in the four most abundant genera of *Archaea* detected in our reactors, which is in accordance with previous studies from similarly operated AD (Blume *et al.*, 2010; Sasaki *et al.*, 2011; Hagen *et al.*, 2014; Tuan *et al.*, 2014; Ziganshina *et al.*, 2014).

The abundance of *Archaea* (1–2%) was relatively low, compared with *Bacteria* (98–99%). Several previous studies of the microbial diversity in AD are based on separate analysis for *Archaea* and *Bacteria*, and the abundance of the two is thus not directly comparable (Patil *et al.*, 2010; Kim *et al.*, 2011; Lee *et al.*, 2012; Rodríguez *et al.*, 2012). Although we applied a universal primer set targeting both kingdoms, the abundance count of *Archaea* can be biased because of extraction and PCR. The approach used in this study does not take account of the 16S ribosomal RNA gene copy number, which has previously been shown to be generally lower in *Archaea* than *Bacteria* (Lee *et al.*, 2009). However, the abundance ratio of *Archaea* and *Bacteria* is in accordance with the metagenome.

Time, rather than the two different concentrations of acetate tested, was the cause of the observed fluctuations in the community structures. A significant increase in *Bacillales*, specifically the genera *Ureibacillus*, was observed. Although the abundance of the genera of *Ureibacillus* can potentially be attributed to the presence of acetate, no incorporation of ^{13}C from acetate was observed at protein level.

The abundances of *Methanobrevibacter* and *Methanoculleus* were constant during the incubation, the abundance of *Methanobacterium* decreased,

and the abundance of *Methanosarcina* increased. The small increase of *Methanosarcina* is interesting because this organism is capable of both acetoclastic (Liu *et al.*, 1985) and hydrogenotrophic (Thauer *et al.*, 2008) pathways. Members of *Methanosarcina* are favored at acetate concentrations higher than 1 mM (Karakashev *et al.*, 2006; Hori *et al.*, 2011), although the biochemical reasoning remains unknown.

The microorganisms directly involved in acetate turnover were investigated with protein-SIP, not only identifying the microorganisms but also determining their level of activity. ^{13}C-labeled peptides were detected only in the reactors fed with high concentrations of acetate; a reason for this could be a higher turnover rate of acetate of fewer specialized organisms and/or the relative high levels of labeling required for isotopical profiling. The focus hereafter will be on samples from the 100 mM reactor. ^{13}C isotopically labeled peptides of the microorganisms were observed after 48 h of incubation (five peptides). The number of identified labeled peptides increased over time (56 peptides after 192 h), indicating that an adaptation period, for example, protein synthesis, for the microorganisms toward a change in environmental conditions was required.

The number of ^{13}C-labeled peptides identified increased by using the Foulum metagenome as a reference database. Still, the number of ^{13}C-labeled peptides detected in our reactors is low and can be explained by the very dense nature of the samples and the fact that protein extractions are often contaminated with humic substances, which, in correlation with a bias of mass spectrometry toward the most abundant proteins, challenges subsequent isotopical profiling (Doherty and Beynon, 2006; Heyer *et al.*, 2013). Furthermore, the microbial communities in the AD are very complex, hence difficult to analyze using mass spectrometry. However, we detected between 1000 and 2100 unlabeled peptides in our reactors, which is a much greater number than those labeled with ^{13}C, the incubation for a total of 9 days may have been too short for the slow-growing methanogens to adjust and synthesize new proteins, causing insufficient labeling.

Peptides from five subspecies of *Clostridia* (C1–C5), as well as *Methanosarcina* and *Methanoculleus* (M), incorporated ^{13}C from the reactors fed with high levels of ^{13}C-labeled acetate. Methyl coenzyme M reductase from *Methanosarcina barkeri* was ^{13}C labeled, which is involved in methanogenesis, both acetoclastic and hydrogenotrophic. However, many of the peptides came from household proteins and were not directly involved in the SAO pathway. Formyltetrahydrofolate synthetase catalyzes the formation of acetate from H_2 and CO_2 (Xu *et al.*, 2009; Hori *et al.*, 2011), but has previously been associated with SAO in AD (Hori *et al.*, 2011). The gene encoding the enzyme formyltetrahydrofolate synthetase, *fthfs*, is an ecological biomarker for reductive acetogenesis (Xu *et al.*, 2009; Hori *et al.*, 2011). Thus, we searched for *fthfs* in the six-frame translated Foulum metagenome, which was present in all of the *Bacteria* detected with the ^{13}C-labeling approach. However, only two of the remaining marker genes, *acsC* and *acsD*, encoding CO dehydrogenase/acetyl-CoA synthase subunits.

Despite the absence of these genes, protein-SIP data suggest that these phylotypes are responsible for SAO. Most of the ^{13}C-labeled proteins affiliated with the genus *Gelria* (c1). The enzymes of the Wood–Ljungdahl pathway are generally poorly understood for SAOB, and it has previously been suggested that other metabolic strategies than the Wood–Ljungdahl are being used by SAOB (Müller *et al.*, 2013).

Most of the ^{13}C-labeled peptides had a RIA (proportion of the peptide ^{13}C labeled) of around 13–36%, however, four peptides had higher RIA values of 49.6% and 51.7% (*Methanoculleus*), 58.1% (*Methanosarcina*), and 93.8% (genus *Gelria* in the class *Clostridia*), respectively. The LR (how much of a peptide population is labeled) of these four peptides were 2.3% and 2.8% (*Methanoculleus*), and 39.2% (*Methanosarcina*) and 35.0% (*Gelria*). These data clearly confirm that these microorganisms are part of acetate degradation.

We detected unlabeled peptides from several methanogens, both acticlastic and hydrogenotrophic. Among the methanogens, *Methanosarcina* had the highest ^{13}C labeling with a RIA of 58.1% and an LR of 39.2%. The labeled peptide came from the methyl coenzyme M reductase β subunit, which is a common intermediate reaction of all metabolic pathways leading to methane formation (Grabarse *et al.*, 2001). Thus, methyl coenzyme M reductase takes part in both methanogenic pathways (Rademacher *et al.*, 2012). The highest ^{13}C labeling of *Methanosarcina* is in accordance with the measured acetate consumption rate and the observed increase in the relative abundance of *Methanosarcina* during the course of incubation, as shown by the amplicon sequencing analysis. This methanogen participates in acid recovery in ADs by transformation of acetate in accordance with previous studies (Petersen, 1991). *Methanosarcina* was also highly abundant in the reactor fed with 100 mM [2-^{13}C] acetate presented in our previous study, and the results of the isotope analysis demonstrated the key role of SAO-HM in the degradation of acetate (Mulat *et al.*, 2014).

Adjusting the parameters of the AD to favor the presence and activity, *Methanosarcina* can possibly improve the stability of the reactor as this organism is able to carry out both acetoclastic and hydrogenotrophic methanogenesis and is more tolerant of several inhibitors such as ammonium, low retention times and high organic loading rates (De Vrieze *et al.*, 2012). *Methanosaeta*, which are strictly acetoclastic methanogens, were not detected with amplicon sequencing. This could point in the direction of SAO-HM being the dominant process. This pathway

is similarly dominant at thermophilic temperatures and in plants with increased levels of acetate (De Vrieze *et al.*, 2012). However, as *Methanosarcina* is capable of both methanogenesis pathways, it is not possible to define the dominant pathway in the digester under high acetate levels.

Methanoculleus was the other methanogen found with labeled peptides. This particular methanogen is hydrogenotrophic and grows on H_2 and CO_2 (Mikucki *et al.*, 2003). Applying [1-^{13}C]acetate and [2-^{13}C]acetate would allow to differentiate between acetoclastic or hydrogenotrophic methanogenesis. Furthermore, the use of primers targeting the *fthfs* gene would allow us to identify the specific SAOB present in our reactors. As *Methanoculleus* incorporated ^{13}C into their peptides while growing on 100 mM [2-^{13}C]acetate, they likely use the SAO-HM pathway in syntrophy with SAOB.

Conclusion

In this study, we showed that protein-SIP is a method that can be used to detect the active microorganisms incorporating ^{13}C into their proteins in complex samples from AD batch reactors. We conclude that the mapping of protein-SIP onto a binned metagenome is highly applicable for identifying members of functional groups in complex microbial ecosystems. Peptides from *Clostridia*, *Methanosarcina* and *Methanoculleus* were labeled with ^{13}C and therefore confirmed that these microorganisms were involved in the recovery after inhibitory events with high levels of acetate. The ^{13}C-labeled and identified *Clostridia* are most likely oxidizing acetate as part of a synthrophy as they all contain the *fthfs* gene coding for formyltetrahydrofolate synthetase, a key enzyme in reductive acetogenesis. The findings therefore strongly indicate that these cells are new SAOB that can facilitate acetate consumption via SAO, coupled with hydrogenotrophic methanogenesis (SAO-HM). As *Methanosarcina* is a mixotrophic methanogen, its exact role as acetoclastic or hydrogenotrophic methanogenesis was not verified. *Methanoculleus* are hydrogenotrophic and thus likely involved in SAO-HM pathway under conditions with high concentrations of acetate.

Conflict of Interest

The authors declare no conflict of interest.

Acknowledgements

References

Albertsen M, Hugenholtz P, Skarshewski A, Nielsen KL, Tyson GW, Nielsen PH. (2013). Genome sequences of rare, uncultured bacteria obtained by differential coverage binning of multiple metagenomes. *Nat Biotechnol* **31**: 533–538.

Angelidaki I, Ahring BK. (1993). Thermophilic anaerobic digestion of livestock waste: the effect of ammonia. *Appl Microbiol Biotechnol* **38**; 560–564.

Balk M, Weijma J, Stams AJM. (2002). Thermotoga lettingae sp. nov., a novel thermophilic, methanol-degrading bacterium isolated from a thermophilic anaerobic reactor. *Int J Syst Evol Microbiol* **52**: 1361–1368.

Bastida F, Rosell M, Franchini AG, Seifert J, Finsterbusch S, Jehmlich N *et al.* (2010). Elucidating MTBE degradation in a mixed consortium using a multidisciplinary approach. *FEMS Microbiol Ecol* **73**: 370–384.

Blume F, Bergmann I, Nettmann E, Schelle H, Rehde G, Mundt K *et al.* (2010). Methanogenic population dynamics during semi-continuous biogas fermentation and acidification by overloading. *J Appl Microbiol* **109**: 441–450.

Botelho D, Wall MJ, Vieira DB, Fitzsimmons S, Liu F, Doucette A. (2010). Top-down and bottom-up proteomics of SDS-containing solutions following mass-based separation. *J Proteome Res* **9**: 2863–2870.

Can M, Armstrong FA, Ragsdale SW. (2014). Structure, function, and mechanism of the nickel metalloenzymes, CO dehydrogenase, and acetyl-CoA synthase. *Chem Rev* **114**: 4149–4174.

Chen Y, Cheng JJ, Creamer KS. (2008). Inhibition of anaerobic digestion process: a review. *Bioresource Technol* **99**: 4044–4064.

De Vrieze J, Hennebel T, Boon N, Verstraete W. (2012). Methanosarcina: the rediscovered methanogen for heavy duty biomethanation. *Bioresource Technol* **112**: 1–9.

Demirel B, Yenigün O. (2002). Two-phase anaerobic digestion processes: a review. *J Chem Technol Biotechnol* **77**: 743–755.

Doherty MK, Beynon RJ. (2006). Protein turnover on the scale of the proteome. *Exp Rev Proteomics* **3**: 97–110.

Ermler U. (1997). Crystal structure of methyl-coenzyme M reductase: the key enzyme of biological methane formation. *Science* **278**: 1457–1462.

Finn RD, Bateman A, Clements J, Coggill P, Eberhardt RY, Eddy SR *et al.* (2014). Pfam: the protein families database. *Nucl Acids Res* **42**: D222–D230.

Fotidis IA, Karakashev D, Angelidaki I. (2013). Bioaugmentation with an acetate-oxidising consortium as a tool to tackle ammonia inhibition of anaerobic digestion. *Bioresource Technol* **146**: 57–62.

Grabarse W, Mahlert F, Duin EC, Goubeaud M, Shima S, Thauer RK *et al.* (2001). On the mechanism of biological methane formation: structural evidence for conformational changes in methyl-coenzyme M reductase upon substrate binding. *J Mol Biol* **309**: 315–330.

Hagen LH, Vivekanand V, Linjordet R, Pope PB, Eijsink VGH, Horn SJ. (2014). Microbial community structure and dynamics during co-digestion of whey permeate and cow manure in continuous stirred tank reactor systems. *Bioresource Technol* **171**: 350–359.

Hansen SH, Stensballe A, Nielsen PH, Herbst F-A. (2014). Metaproteomics: evaluation of protein extraction from activated sludge. *Proteomics* **14**: 2535–2539.

Hao L, Lü F, Mazéas L, Desmond-Le Quéméner E, Madigou C, Guenne A *et al.* (2014). Stable isotope probing of acetate fed anaerobic batch incubations shows a partial resistance of acetoclastic methanogenesis catalyzed by Methanosarcina to sudden increase of ammonia level. *Water Res* **69C**: 90–99.

Hattori S, Kamagata Y, Hanada S, Shoun H. (2000). Thermacetogenium phaeum gen. nov., sp. nov., a strictly anaerobic, thermophilic, syntrophic acetate-oxidizing bacterium. *Int J Syst Evol Microbiol* **50**(Pt 4): 1601–1609.

Hattori S. (2008). Syntrophic acetate-oxidizing microbes in methanogenic environments. *Microbes Environ* **23**: 118–127.

Herbst F-A, Bahr A, Duarte M, Pieper DH, Richnow H-H, von Bergen M *et al.* (2013). Elucidation of *in situ* polycyclic aromatic hydrocarbon degradation by functional metaproteomics (protein-SIP). *Proteomics* **13**: 2910–2920.

Heyer R, Kohrs F, Benndorf D, Rapp E, Kausmann R, Heiermann M *et al.* (2013). Metaproteome analysis of the microbial communities in agricultural biogas plants. *New Biotechnol* **30**: 614–622.

Hori T, Sasaki D, Haruta S, Shigematsu T, Ueno Y, Ishii M *et al.* (2011). Detection of active, potentially acetate-oxidizing syntrophs in an anaerobic digester by flux measurement and formyltetrahydrofolate synthetase (FTHFS) expression profiling. *Microbiology (Reading, England)* **157**: 1980–1989.

Ito T, Yoshiguchi K, Ariesyady HD, Okabe S. (2011). Identification of a novel acetate-utilizing bacterium belonging to Synergistes group 4 in anaerobic digester sludge. *ISME J* **5**: 1844–1856.

Jehmlich N, Schmidt F, Taubert M, Seifert J, Bastida F, von Bergen M *et al.* (2010). Protein-based stable isotope probing. *Nat Protocols* **5**: 1957–1966.

Jehmlich N, Schmidt F, von Bergen M, Richnow H-H, Vogt C. (2008). Protein-based stable isotope probing (Protein-SIP) reveals active species within anoxic mixed cultures. *ISME J* **2**: 1122–1133.

Karakashev D, Batstone DJ, Trably E, Angelidaki I. (2006). Acetate oxidation is the dominant methanogenic pathway from acetate in the absence of Methanosaetaceae. *Appl Environ Microbiol* **72**: 5138–5141.

Kim J, Shin SG, Han G, O'Flaherty V, Lee C, Hwang S. (2011). Common key acidogen populations in anaerobic reactors treating different wastewaters: molecular identification and quantitative monitoring. *Water Res* **45**: 2539–2549.

Kjeldal H, Pell L, Pommerening-Röser A, Nielsen JL. (2014). Influence of p-cresol on the proteome of the autotrophic nitrifying bacterium Nitrosomonas eutropha C91. *Arch Microbiol* **196**: 497–511.

Kleindienst S, Herbst F-A, Stagars M, von Netzer F, von Bergen M, Seifert J *et al.* (2014). Diverse sulfate-reducing bacteria of the Desulfosarcina/Desulfococcus clade are the key alkane degraders at marine seeps. *ISME J* **8**: 2029–2044.

Klocke M, Mähnert P, Mundt K, Souidi K, Linke B. (2007). Microbial community analysis of a biogas-producing completely stirred tank reactor fed continuously with fodder beet silage as mono-substrate. *Syst Appl Microbiol* **30**: 139–151.

Kohlbacher O, Reinert K, Gröpl C, Lange E, Pfeifer N, Schulz-Trieglaff O *et al.* (2007). TOPP–the OpenMS proteomics pipeline. *Bioinforma Oxf Engl* **23**: e191–e197.

Krakat N, Schmidt S, Scherer P. (2011). Potential impact of process parameters upon the bacterial diversity in the mesophilic anaerobic digestion of beet silage. *Bioresource Technol* **102**: 5692–5701.

Labatut RA, Angenent LT, Scott NR. (2014). Conventional mesophilic vs. thermophilic anaerobic digestion: a trade-off between performance and stability? *Water Res* **53**: 249–258.

Lee S-H, Kang H-J, Lee YH, Lee TJ, Han K, Choi Y *et al.* (2012). Monitoring bacterial community structure and variability in time scale in full-scale anaerobic digesters. *J Environ Monitor* **14**: 1893–1905.

Lee ZM-P, Bussema C, Schmidt TM. (2009). rrnDB: documenting the number of rRNA and tRNA genes in bacteria and archaea. *Nucleic Acids Res* **37**: D489–D493.

Liu Y, Boone DR, Sleat R, Mah RA. (1985). Methanosarcina mazei LYC, a new methanogenic isolate which produces a disaggregating enzyme. *Appl Environ Microbiol* **49**: 608–613.

Lovell CR, Leaphart AB. (2005). Community-level analysis: key genes of CO2-reductive acetogenesis. *Methods Enzymol* **397**: 454–469.

Lü F, Hao L, Guan D, Qi Y, Shao L, He P. (2013). Synergetic stress of acids and ammonium on the shift in the methanogenic pathways during thermophilic anaerobic digestion of organics. *Water Res* **47**: 2297–2306.

Manzoor S, Müller B, Niazi A, Bongcam-Rudloff E, Schnürer A. (2013). Draft genome sequence of Clostridium ultunense strain esp, a syntrophic acetate-oxidizing bacterium. *Genome Announcements* **1**: e0010713.

Mikucki JA, Liu Y, Delwiche M, Colwell FS, Boone DR. (2003). Isolation of a methanogen from deep marine sediments that contain methane hydrates, and description of Methanoculleus submarinus sp. nov. *Appl Environ Microbiol* **69**: 3311–3316.

Mulat DG, Ward AJ, Adamsen APS, Voigt NV, Nielsen J, Feilberg A. (2014). Quantifying contribution of synthrophic acetate oxidation to methane production in thermophilic anaerobic reactors by membrane inlet mass spectrometry. *Environ Sci Technol* **48**: 2505–2511.

Müller B, Sun L, Schnürer A. (2013). First insights into the syntrophic acetate-oxidizing bacteria–a genetic study. *Microbiol Open* **2**: 35–53.

Palatsi J, Viñas M, Guivernau M, Fernandez B, Flotats X. (2011). Anaerobic digestion of slaughterhouse waste: main process limitations and microbial community interactions. *Bioresource Technol* **102**: 2219–2227.

Patil SS, Kumar MS, Ball AS. (2010). Microbial community dynamics in anaerobic bioreactors and algal tanks treating piggery wastewater. *Appl Microbiol Biotechnol* **87**: 353–363.

Petersen S. (1991). Acetate oxidation in a thermophilic anaerobic sewage-sludge digestor: the importance of non-aceticlastic methanogenesis from acetate. *FEMS Microbiol Lett* **86**: 149–152.

Rademacher A, Zakrzewski M, Schlüter A, Schönberg M, Szczepanowski R, Goesmann A *et al.* (2012). Characterization of microbial biofilms in a thermophilic biogas system by high-throughput metagenome sequencing. *FEMS Microbiol Ecol* **79**: 785–799.

Rajagopal R, Massé DI, Singh G. (2013). A critical review on inhibition of anaerobic digestion process by excess ammonia. *Bioresource Technol* **143**: 632–641.

Rodríguez E, Lopes A, Fdz-Polanco M, Stams AJM, García-Encina PA. (2012). Molecular analysis of the biomass of a fluidized bed reactor treating synthetic vinasse at anaerobic and micro-aerobic conditions. *Appl Microbiol Biotechnol* **93**: 2181–2191.

Sachsenberg T, Herbst F-A, Taubert M, Kermer R, Jehmlich N, von Bergen M *et al.* (2015). MetaProSIP: automated inference of stable isotope incorporation rates in proteins for functional metaproteomics. *J Proteome Res* **14**: 619–627.

Sasaki D, Hori T, Haruta S, Ueno Y, Ishii M, Igarashi Y. (2011). Methanogenic pathway and community structure in a thermophilic anaerobic digestion process of organic solid waste. *J Biosci Bioeng* **111**: 41–46.

Schlüter A, Bekel T, Diaz NN, Dondrup M, Eichenlaub R, Gartemann K-H *et al.* (2008). The metagenome of a biogas-producing microbial community of a production-scale biogas plant fermenter analysed by the 454-pyrosequencing technology. *J Biotechnol* **136**: 77–90.

Schnürer A, Schink B, Svensson BH. (1996). Clostridium ultunense sp. nov., a mesophilic bacterium oxidizing acetate in syntrophic association with a hydrogenotrophic methanogenic bacterium. *Int J Syst Bacteriol* **46**: 1145–1152.

Seifert J, Herbst F-A, Halkjaer Nielsen P, Planes FJ, Jehmlich N, Ferrer M *et al.* (2013). Bioinformatic progress and applications in metaproteogenomics for bridging the gap between genomic sequences and metabolic functions in microbial communities. *Proteomics* **13**: 2786–2804.

Shevchenko A, Tomas H, Havlis J, Olsen J V, Mann M. (2006). In-gel digestion for mass spectrometric characterization of proteins and proteomes. *Nat Protocols* **1**: 2856–2860.

St-Pierre B, Wright A-DG. (2014). Comparative metagenomic analysis of bacterial populations in three full-scale mesophilic anaerobic manure digesters. *Appl Microbiol Biotechnol* **98**: 2709–2717.

Sturm M, Bertsch A, Gröpl C, Hildebrandt A, Hussong R, Lange E *et al.* (2008). OpenMS - an open-source software framework for mass spectrometry. *BMC Bioinformatics* **9**: 163.

Sundberg C, Al-Soud WA, Larsson M, Alm E, Yekta SS, Svensson BH *et al.* (2013). 454 pyrosequencing analyses of bacterial and archaeal richness in 21 full-scale biogas digesters. *FEMS Microbiol Ecol* **85**: 612–626.

Taubert M, Jehmlich N, Vogt C, Richnow HH, Schmidt F, von Bergen M *et al.* (2011). Time resolved protein-based stable isotope probing (protein-SIP) analysis allows quantification of induced proteins in substrate shift experiments. *Proteomics* **11**: 2265–2274.

Taubert M, Vogt C, Wubet T, Kleinsteuber S, Tarkka MT, Harms H *et al.* (2012). Protein-SIP enables time-resolved analysis of the carbon flux in a sulfate-reducing, benzene-degrading microbial consortium. *ISME J* **6**: 2291–2301.

Thauer RK, Kaster A-K, Seedorf H, Buckel W, Hedderich R. (2008). Methanogenic archaea: ecologically relevant differences in energy conservation. *Nat Rev Microbiol* **6**: 579–591.

Tuan NN, Chang Y-C, Yu C-P, Huang S-L. (2014). Multiple approaches to characterize the microbial community in a thermophilic anaerobic digester running on swine manure: a case study. *Microbiol Res* **169**: 717–724.

Vizcaíno JA, Deutsch EW, Wang R, Csordas A, Reisinger F, Ríos D *et al.* (2014). ProteomeXchange provides globally coordinated proteomics data submission and dissemination. *Nat Biotechnol* **32**: 223–226.

Westerholm M, Roos S, Schnürer A. (2010). Syntrophaceticus schinkii gen. nov., sp. nov., an anaerobic, syntrophic acetate-oxidizing bacterium isolated from a mesophilic anaerobic filter. *FEMS Microbiol Lett* **309**: 100–104.

Westerholm M, Roos S, Schnürer A. (2011). Tepidanaerobacter acetatoxydans sp. nov., an anaerobic, syntrophic acetate-oxidizing bacterium isolated from two ammonium-enriched mesophilic methanogenic processes. *Syst Appl Microbiol* **34**: 260–266.

Wirth R, Kovács E, Maróti G, Bagi Z, Rákhely G, Kovács KL. (2012). Characterization of a biogas-producing microbial community by short-read next generation DNA sequencing. *Biotechnol Biofuels* **5**: 41.

Xu K, Liu H, Du G, Chen J. (2009). Real-time PCR assays targeting formyltetrahydrofolate synthetase gene to enumerate acetogens in natural and engineered environments. *Anaerobe* **15**: 204–213.

Ziganshina EE, Bagmanova AR, Khilyas I V, Ziganshin AM. (2014). Assessment of a biogas-generating microbial community in a pilot-scale anaerobic reactor. *J Biosci Bioeng* **117**: 730–736.

Supplementary Information accompanies this paper on The ISME Journal website (http://www.nature.com/ismej)